ELSEVIER

Micron 36 (2005) 617–629

micron

www.elsevier.com/locate/micron

Review

Micro- and nano-structural analyses of damage in bone

Nadder D. Sahar[a], Sun-Ig Hong[b], David H. Kohn[a,c,*]

[a]*Biomedical Engineering, University of Michigan, Ann Arbor, MI 48109–1078, USA*
[b]*Metallurgical Engineering, Chungnam National University, Taejon 305-764, South Korea*
[c]*Department of Biologic and Materials Sciences, University of Michigan, Ann Arbor, MI 48109–1078 USA*

Abstract

Skeletal fractures represent a significant medical and economic burden for our society. In the US alone, age-related hip, spine, and wrist fractures accounted for more than $17 billion in direct health care costs in 2001. Moreover, skeletal fractures are not limited to the elderly; stress fractures and impact/trauma-related fractures are a significant problem in younger people also. Gaining insight into the mechanisms of fracture and how these mechanisms are modulated by intrinsic as well as extrinsic factors may improve the ability to define fracture risk and develop and assess preventative therapies for skeletal fractures. Insight into failure mechanisms of bone, particularly at the ultrastructural-level, is facilitated by the development of improved means of defining and measuring tissue quality. Included in these means are microscopic and spectroscopic techniques for the direct observation of crack initiation, crack propagation, and fracture behavior. In this review, we discuss microscopic and spectroscopic techniques, including laser scanning confocal microscopy (LSCM), scanning electron microscopy (SEM), transmission electron microscopy (TEM) and Raman spectroscopic imaging for visually observing microdamage in bone, and the current understanding of damage mechanisms derived from these techniques.

Keywords: Bone; Microdamage; Fatigue; Laser scanning confocal microscopy; Scanning electron microscopy; Transmission electron microscopy; Raman spectroscopy

Contents

* Corresponding author. Address: Department of Biologic and Materials Sciences, University of Michigan, 1011 North University Avenue, Ann Arbor, MI 48109–1078, USA. Tel.: +1 734 764 2206; fax: +1 734 647 2110.
E-mail address: dhkohn@umich.edu (D.H. Kohn).

0968-4328/$ - see front matter © 2005 Elsevier Ltd. All rights reserved.
doi:10.1016/j.micron.2005.07.006

1. Introduction

1.1. Clinical importance of damage—skeletal fragility

Skeletal fractures represent a significant medical and economic burden for our society (Hui et al., 1988; Burr and Milgrom, 2001; Burr, 1997; Praemer et al., 1999). In the US alone, age-related hip, spine, and wrist fractures accounted for more than $17 billion in direct health care costs in 2001, and this annual cost is rising (National Osteoporosis Foundation, 2001). It is estimated that the number of Americans that will have osteoporosis by 2015 could be in excess of 41 million, a third more than the 28 million currently affected by the disease. Moreover, skeletal fractures are not limited to the elderly—stress fractures and impact/trauma-related fractures are a clinically significance problem in younger people also. For example, approximately half a million long distance runners present with stress fractures each year, and over 20% of 'competitive' runners incur stress fractures (Burr and Milgrom, 2001; Bennell et al., 1996). A significant percentage of military recruits, particularly females, exhibits stress fractures, and a significantly greater percentage of the military population exhibits stress fractures compared to the general population (Burr and Milgrom, 2001; Jones et al., 1989). It is generally thought that a high incidence of musculoskeletal fatigue loading results in damage accumulation at too high of a rate to be efficiently remodeled, leading to skeletal fracture (Jordaan and Schwellnus, 1994; Beck et al., 2000).

Gaining insight into the underlying mechanisms of fracture and how these mechanisms are modulated by intrinsic (e.g. aging, disease) as well as extrinsic (e.g. mechanical loading) factors may improve the ability to define fracture risk and develop and assess preventative therapies for skeletal fractures. It is generally accepted that age-related fractures result from not only a loss in bone mass, but also because of alterations in tissue quality, such as reduced elasticity of the organic phase resulting from changes in collagen cross-linking, and altered mineral composition and crystal structure (Burr et al., 1997; Rajachar, 2003). Therefore, it is important to also delineate changes in tissue quality and how these changes in tissue ultrastructure affect the mechanistic response of bone to its physical environment. Insight into failure mechanisms of bone, particularly at the ultrastructural-level, is facilitated by the development of improved means of defining and measuring tissue quality. Included in these means are microscopic and spectroscopic techniques for direct observation of crack initiation, propagation, and fracture behavior.

1.2. Microdamage as an indicator of skeletal fragility

Repetitive mechanical loading can lead to ultrastructural-level damage, the most prevalent form being discrete microcracks in the bone extracellular matrix that are easily visible under brightfield light microscopy (Burr and Milgrom, 2001; Burr et al., 1997; Courtney et al., 1996; Currey et al., 1996; Zioupos and Currey, 1998; Schaffler et al., 1995). Even though younger people are more active and subject to repetitive loading of greater magnitude and duration, they typically have a greater physiologic capacity to withstand the functional demands placed on the musculoskeletal system, and microdamage is repaired by remodeling. However, with age and/or pathologic conditions, the compensatory mechanisms needed to maintain the mechanical stability of skeletal tissue become impaired (Birdwood, 1996). As a result, ultrastructural-level damage, which may no longer be repaired as efficiently, can play a role in the etiology of osteoporotic and stress fractures (Burr and Milgrom, 2001; Burr, 1997; Jones et al., 1989; Burr et al., 1997; Schaffler et al., 1995).

There is therefore an inter-relationship between fatigue loading, microdamage accumulation, remodeling, bone matrix repair and fracture (Fig. 1), and should damage processes exceed the local capacity of tissue to remodel (through either true greater net damage or compromised repair), fracture occurs. Remodeling is triggered by microdamage accumulation, through cell sensory mechanisms, leading to bone matrix repair. However, sometimes remodeling can also enhance microdamage accumulation or directly lead to fracture upon exceeding a threshold stress. Locally, because there is less bone to sustain loading upon resorption induced by remodeling, strains on the remaining bone would increase, generating even more microdamage, which stimulates another sequence of remodeling and so forth (Burr et al., 1997). Therefore high remodeling as well as microdamage accumulation can lead to fracture.

Distributions of sub-threshold microcracks increase exponentially in number with age (Schaffler et al., 1995). These cracks range in length up to 300 μm and may ultimately contribute to age-related property degradation and fatigue fracture in skeletally mature cortical and trabecular bone (Schaffler et al., 1995). Most microcracks form preferentially at cement lines and inter-lamellar boundaries, where one might expect planes of weakness. Vashishth et al. (2000a) provided a detailed account of microcrack formation and contribution towards the propagation of a fracture crack, and showed that the basic fractured element is a mineralized collagen fibril. The processes guiding the location, orientation, size and rate of

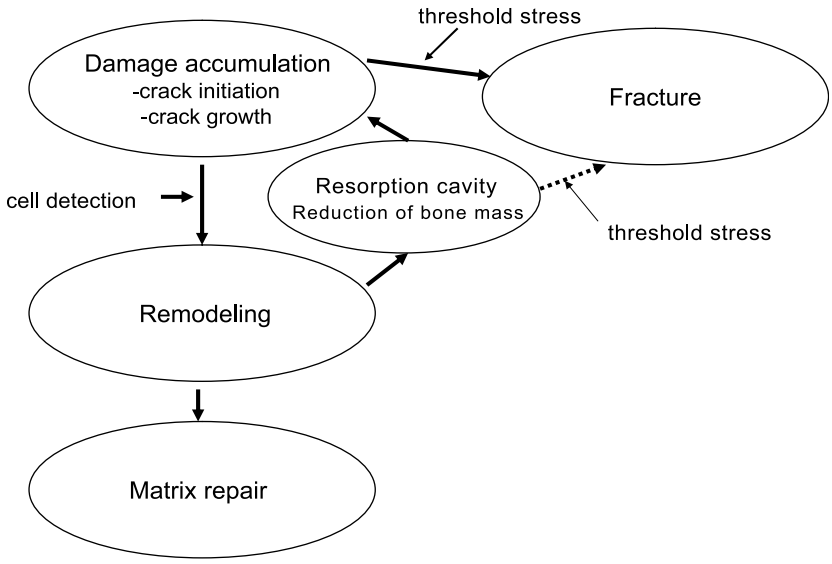

Fig. 1. Schematic of relationship between microdamage, bone remodeling and fracture. Microdamage accumulation can provide a stimulus for intracortical bone remodeling and matrix repair or, beyond a certain threshold, damage exceeds repair and fracture occurs.

microdamage accumulation and the relationships between these damage parameters and ultrastructural constituents are therefore important in assessing the competence of skeletal tissues. To better understand these processes, an ability to accurately detect and measure microdamage is essential. In the following sections, we discuss microscopic and spectroscopic techniques, including laser scanning confocal microscopy (LSCM), scanning electron microscopy (SEM), transmission electron microscopy (TEM) and Raman spectroscopic imaging for visually observing microdamage in bone, and the current understanding of damage mechanisms derived from these techniques.

2. Observations of microdamage at the light and confocal microscopic levels and insight developed

2.1. Identifying different types of microdamage

The most common technique for viewing microdamage in bone generated in-vivo or controlled in-vitro testing is optical microscopy. However, sectioning and grinding specimens to make slides suitable for observing microdamage can create artifactual microdamage. Frost (1960) addressed this problem by bulk staining bone with basic fuchsin before sectioning. Fuchsin stains all surfaces of bone, including lacunae, canaliculi, blood vessels, and microdamage. Therefore, damage that existed before processing will be stained, while processing-induced damage will not be. Using this technique, Frost (1960) was able to show that microdamage does exist in vivo, indicating that repetitive physiological loads are sufficient to create small-scale damage in bone. Burr and Stafford (1990) later validated this method, finding that the dehydration steps of the staining protocol do not create additional damage, and pre-existing damage can be discriminated from artifactual damage.

Using bulk staining techniques, two main types of damage have been found in bone: microcracks and diffuse microdamage. Microcracks are clear, distinguishable, linear cracks (at least in the plane of the 2D section being viewed), while diffuse damage appears as a cloud of stain with indistinguishable individual features. Since microcracks and other forms of microdamage are 3D entities, but are being viewed in specific 2D planes, explicit identification and quantification are not always straightforward. Burr and Stafford (1990) therefore developed criteria for identifying microcracks. Microcracks have sharp borders surrounded by a halo of stain, are larger than canaliculi and smaller than vascular canals, are stained through the depth of the section, and have well stained edges with less stain in the intervening space.

Although diffuse damage appears as a cloud of stain, it is likely comprised of many tiny cracks, as indicated by higher magnification observations. Diffuse damage may have a fractal nature to it; as magnification and resolution are increased, more and more cracks become visible in the network of cracks that create the damage pattern.

Recently, laser scanning confocal microscopy (LSCM) has been used to view microdamage (Fazzalari et al., 1998; Boyce et al., 1998; Rajachar, 2003) (Fig. 2). This technique has two advantages over light microscopy. First, only stained surfaces are imaged, making it easier to separate preexisting damage from processing-induced damage. Second, LSCM creates a thin plane of focus that can be panned up and down through the specimen. Having microstructural information in the third dimension is helpful in better characterizing microdamage and distinguishing it from native features in bone, and also allows for 3D reconstruction of images. Using LSCM to characterize

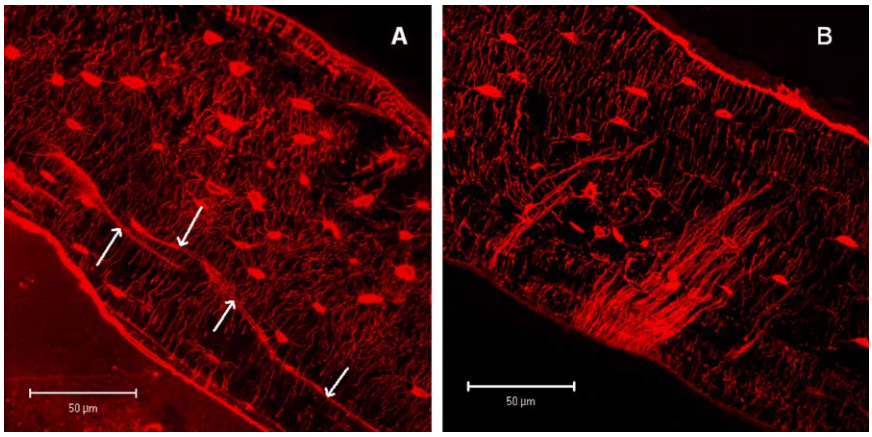

Fig. 2. Laser scanning confocal microscope images of murine cortical bone subjected to fatigue under four-point bending. In the compressive region (A), long linear microcracks are present (indicated by arrows). In the tensile region (B), there is a cloudy network of tiny cracks that is classified as diffuse damage (60×)
.

different types of damage in 3D, microcracks are observed to be sheet-like and diffuse damage consists of a fine network of smaller cracks ('ultra-microcracks') (Fazzalari et al., 1998; Boyce et al., 1998).

2.2. Initiation and propagation of microdamage

Using bulk-staining techniques, relationships between mechanical history and spatial patterns of damage have been addressed. These different types of damage often appear in specific locations within a bone. In bones subjected to bending, linear microcracks regularly appear in regions subjected to compressive strains, while diffuse microdamage appears in tensile zones (Carter and Hayes, 1977a; Boyce et al., 1998; Reilly and Currey, 2000; Rajachar, 2003) (e.g. Fig. 2). 'Whispy-appearing' cracks near the neutral axis of specimens fatigued in bending have also been found (Boyce et al., 1998).

Most microdamage is found in interstitial bone (Schaffler et al., 1995; O'Brien et al., 2003). Interstitial bone is older than bone located in osteons, because it was formed prior to the remodeling that created the osteons. It is possible that the older bone is more susceptible to damage (e.g. because of altered mineral and/or collagen). Alternatively, it is possible that this bone contains more damage because it has been subjected to more loading cycles. Although most microdamage initiates in interstitial bone, it seldom crosses cement lines and into osteons, leading to the hypothesis that cement lines arrest crack growth (Norman and Wang, 1997). An exception to this trend is the whispy-appearing cracks, which commonly cross cement lines and propagate into osteons (Boyce et al., 1998).

Micro and ultrastructural features of bone can create stress concentrations that initiate crack formation. Frequently, microcracks initiate at osteocyte lacunae, leading to the hypothesis that lacunae serve as stress concentrators (Reilly, 2000; Martin et al., 1998). Besides lacunae, vascular canals can also initiate crack formation (Carter and Hayes, 1977a). In addition to stress concentrations, higher mineralization can increase the probability of microcracking. For example, heavily mineralized bone is stiffer than less mineralized bone, but also more brittle and associated with more microcracks (Sobelman et al., 2004).

Crack growth in bone appears to be self-limiting in tension, but less restricted in compression, indicating strain mode-dependent crack extension (Akkus and Rimnac, 2001; Vashishth et al., 2003; Griffin et al., 1997). Microcracks formed from cyclic tension have decreasing growth rate with increasing length and typically arrest in less than 10,000 cycles (Akkus and Rimnac, 2001). Similarly, crack growth resistance increases with crack extension (Vashishth et al., 2003). Burr et al. (1998) claimed that damage actually accumulates more rapidly in tension than compression, but is limited by slow growth in tension. Collectively, these findings indicate that although microcracks do form under far-field tensile loading, their growth is limited and the cracks remain small. In contrast, microcracks produced in compression tend to be long linear cracks, indicative of more uninhibited growth.

Patterns of diffuse damage can also be explained by these observations. Since microcracks are formed easily in tension, but remain small, a fine network of many tiny cracks is created. In the limit, this network becomes so fine that one crack is indistinguishable from another.

2.3. Mechanical consequences of microdamage

Based on the mechanical behavior of composites, there is an expected association between microdamage accumulation and mechanical property degradation, in particular modulus degradation. However, the specific relationship between these two indicators of damage is unclear. Surprisingly, Burr et al. (1998) did not detect significant microdamage in specimens fatigued in bending until a 15% reduction in elastic modulus was reached, and tensile damage did not reduce bone's energy-absorbing ability until

the elastic modulus was reduced by 20% (Reilly and Currey, 2000). There is debate over whether this finding is universal, or bone and testing condition-specific. It is likely that testing method plays an important role in determining the relationship between damage accumulation and mechanical property degradation (Zioupos, 1999; Burr et al., 1999). For instance, strain rate has an effect on the amount of damage produced and the degree of modulus degradation, and may be just as important as peak strain in determining how much damage will accumulate (Schaffler et al., 1989). Also, the amount and nature of microdamage may differ between uniaxial tension, uniaxial compression, and bending or between fatigue and monotonic testing. Even within a specified testing mode, subtle differences in experimental conditions could change damage processes. For example, in load-control fatigue, some researchers load to a specified initial stress level, while others load to a specified initial strain, calculated to yield a desired initial stress. Because mineralization and elastic modulus differ from bone to bone, mode of testing is an important consideration (i.e. the relationship between stress and strain differs between bones). Another variable that is important in designing a fatigue test is whether the test is conducted under load control or displacement/strain control. In load control, as microdamage accumulates, elastic modulus slowly decreases. When the modulus degrades, loading to the same stress causes each cycle to have a higher peak strain. The result is that after initial modulus loss, samples fatigued in load control will reach failure more rapidly than those fatigued in displacement or strain control.

Left unchecked, fatigue induced microdamage can accumulate and eventually cause fracture. As microdamage accumulates and coalesces, stiffness, ultimate strength and energy to failure are all eventually compromised, resulting in decreased resistance to fracture (Carter and Hayes, 1977b; Danova et al., 2003). Fatigue damage coupled with a progressive loss of stiffness also leads to reduced tensile strength in bone (Carter and Hayes, 1977b). Microdamage can also decrease fracture toughness (Norman et al., 1998) and mechanical energy-absorbing ability (Reilly and Currey, 2000). However, unlike man-made composites, the ability of bone to adapt and self-repair allows for recovery of mechanical properties. For example, rat ulnae fatigued in vivo to 40% stiffness loss exhibited significant decreases in ultimate force and toughness, but 14 days of adaptation recovered all mechanical properties and significantly reduced microdamage (Colopy et al., 2004).

Although microdamage has detrimental effects on bone's mechanical properties, under appropriate conditions, it may also have benefit. For example, microdamage may toughen bone, making it harder to fracture from repetitive loading. A network of microcracks has energy absorbing ability which can dissipate stress and slow crack propagation. Fatigue life can therefore be increased by the presence of microcracks (Sobelman et al., 2004). Vashishth et al. (1997) investigated the propagation of a main crack in bone under tensile fatigue and saw an increase in fracture toughness with increased number of microcracks and extension of a main propagating crack. This group later provided more evidence for a microcrack-based toughening mechanism by identifying microcrack patterns in a frontal process zone and wake of a main propagating crack associated with increased crack growth resistance (Vashishth et al., 2003).

The ability of a microcrack to toughen or embrittle bone may depend on whether toughening is caused by intrinsic properties like microdamage or by extrinsic means, specifically crack bridging. Crack bridging is the formation of unbroken regions of bone in the wake of a crack. These bridges span the crack and prevent it from opening further. It has been argued that this mechanism is the dominant toughening mechanism in bone (Nalla et al., 2004). It may seem confusing that some work has found benefit from microdamage while others show negative effects. One explanation could be the amount of damage that is allowed to accumulate before evaluating mechanical properties. If microdamage does have the ultrastructural benefit of improving mechanical properties such as toughness, it will only be beneficial up to some critical threshold of accumulation. For example, although microcracking can increase fatigue life, cracks exceeding a critical length will grow and ultimately cause failure of the bone (Sobelman et al., 2004). Another consideration is the way in which mechanical properties are tested (i.e. whether properties are derived from monotonic or cyclic testing). The physiological analogue of monotonic testing is a traumatic overload, while fatigue is similar to repetitive loading that occurs during walking, running or various other activities. A controlled amount of damage may help prevent further damage accumulation during normal activity, which, in turn, precludes microdamage from reaching a critical level and causing failure. However, the same amount of microdamage may make the bone more susceptible to fracture by a single traumatic event.

Fracture of bone can therefore occur by one of four mechanisms: traumatic overload (which may or may not be dependent on present microdamage), failure of the ultrastructural toughening mechanism(s), failure of remodeling to prevent a critical amount of microdamage from accumulating, and/or physiological loading so intense that remodeling and toughening cannot prevent accumulation of microdamage.

In summary, microdamage and mechanical properties in bone are generally known to be intertwined, but their specific relationship is not fully understood. The type of microdamage and the way in which it was produced (e.g. in vivo vs. in vitro, uniaxial loading vs. bending, monotonic loading vs. fatigue) will likely change the correlation between damage and mechanical properties. Much remains unclear at this point, but several conclusions are apparent. Microdamage can occur in vivo from physiological loads. Run away extension of microdamage is prevented by a toughening mechanism in which the microdamage can

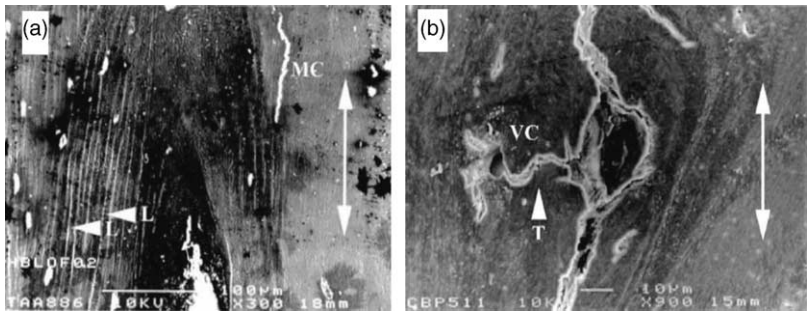

Fig. 3. (a) Failure of longitudinally oriented osteons in human bone. Arrowheads in this micrograph indicate longitudinal microcracks (represented by the letter 'L'); (b) Micrographs demonstrating the presence of stress concentration effects of Volkmann's canals in bovine bone. A transverse microcrack (indicated by an arrowhead and represented by the letter 'T') can be seen connecting the main crack and the Volkmann's canal (VC). In the micrographs, the line with arrowheads at both ends indicates the longitudinal axis of the long bone and the direction in which the main crack (MC) propagated. Reprinted from Vashishth et al., 2000b, with permission from the authors and Elsevier Ltd.

absorb energy from loading. In healthy bone, accumulation of microdamage will initiate remodeling, reducing the amount of damage remaining. Small amounts of microdamage are likely to be stable and not compromise function of bone. To better identify relations between damage, mechanical properties and remodeling, better techniques are needed to detect, monitor and visualize damage, and also relate compositional changes to mechanical and morphological changes.

3. Microdamage analysis using scanning electron microscopy

Bone has a hierarchical composite architecture with various arrangements of material structures at a wide range of length scales that work in concert to perform diverse mechanical, biological and chemical functions (Rho et al., 1998). In order to assess bone architecture, microdamage accumulation and fracture mechanisms, direct observation using various microscopic techniques is necessary. Scanning electron microscopy (SEM) is effective for the analysis of hierarchical composite structure and surface topography induced by microdamage accumulation and fracture because of its high resolution and large depth of field (Hong et al., 1996; Hong and Suryanarayana, 2001; Lee and Hong, 2003). One of the most powerful characteristics of SEM is a great depth of field at all magnifications, which renders the area above and below the focal plane to appear in focus. The depth of field for SEM is 100–500 times greater than the light microscope (Goldstein et al., 1981) and a 3D appearance of the specimen image can be obtained. SEM has been used extensively to study the damage accumulation and fracture behavior of bone (Braidotti et al., 2000; Hiller et al., 2003; Nalla et al., 2003; Schaffler et al., 1994). Ultrastructural level damage in bone which cannot be observed at the light microscopic level can be observed using SEM (Schaffler et al., 1994).

Microdamage in bone can be observed using SEM with or without basic fuchsin staining (Schaffler et al., 1994). Most bone tissue is riddled with voids, in the form of blood channels, erosion cavities, osteocyte lacunae and canaliculi (Currey, 2003), which may act as stress concentrators. The extent to which these stress concentrators increase the likelihood of bone microdamage and fracture is difficult to determine, because the fracture mechanics properties of bone are still not well understood. The arrangement and orientation of these voids in the architecture of bone is complex and these voids in many ways can act as crack deflectors or barriers to crack propagation.

SEM observation of human bone (Vashishth et al., 2000b) indicates that microcracks associated with longitudinally oriented osteons are present in individual lamellae (e.g. Fig. 3(a)). In this figure, longitudinal microcracks are marked with arrowheads and the main crack is marked with 'MC'. The failure of longitudinally oriented osteons in human bone was observed to have two important features (Vashishth et al., 2000b). First, easier microcrack formation and damage localization occur within an osteon due to weak inter-lamellar bonding. Second, formation of microcracks

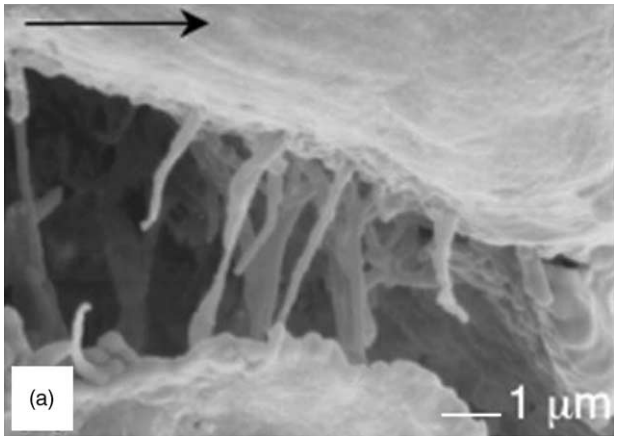

Fig. 4. Scanning electron micrographs of crack bridging by collagen fibers in human cortical bone. The direction of crack propagation is indicated by a black arrow at the top. From Nalla et al., 2003, with copyright permission from Nature (http://www.nature.com/).

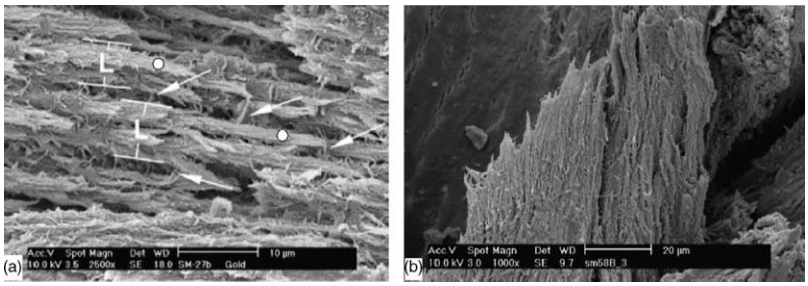

Fig. 5. Details of failure surfaces of bovine subchondral bone: (a) intra-lamellar fiber bundles (dots) belonging to a set of separated lamellae (*L*), connected by short inter-lamellar fibers (arrows), and; (b) pulled-out fiber bundles belonging to a set of undivided lamellae. Reprinted from Braidotti et al., 2000, with permission from the authors and Elsevier Ltd.

occurs at the osteon-matrix interface in the presence of less mineralized cement lines. Crack deflection due to stress concentration effects of Volkmann's canals (e.g. Fig. 3(b)) reduces energy available at the crack tip for extension, and a higher load is required to produce further crack propagation. In the presence of microcracks oriented unfavorably with respect to the main crack, damage is localized and limited, resulting in the deceleration of the main crack propagation (Sobelman et al., 2004; Vashishth et al., 2000b).

Recently, Nalla et al. (2003) examined how a propagating crack interacts with the bone microstructure to provide a mechanistic understanding of fracture using SEM. They suggested that crack bridging by collagen fibers (e.g. Fig. 4), as well as microcracks, contribute to the fracture toughness of bone. Microcracks preferentially form around osteons, leading to matrix debonding or osteon pullout (Nalla et al., 2004). Crack bridging, conversely, involves the formation of unbroken regions that span the crack in the wake of the crack tip and act to resist crack opening. Bridging may occur by unbroken individual collagen fibers and 'uncracked ligaments' (Nalla et al., 2004).

SEM is effective in studying the fracture surface morphology of bone because of the ability to view images in 3D. The most frequently observed features on the fracture surface of lamellar bones are inter-lamellar delamination and layered morphology (e.g. Fig. 5(a)), protruded fiber bundles (e.g. Fig. 5(b)), and osteon pull-out (e.g. Fig. 6) (Braidotti et al., 2000; Weiner et al., 1999; Hiller et al., 2003; Vashishth et al., 2000b). These features observed on the fracture surface reflect the cracking behavior of bone. Inter-lamellar delamination and layer morphology can be associated with the microcracks at the inter-lamellar interfaces and the protruded fiber bundles can be linked to crack bridging by uncracked ligaments and/or collagen fibers. Osteon pull-out is thought to result from shear microcracks along the inter-lamellar interface or cement lines and subsequent osteonal crack bridging (Hiller et al., 2003). It is therefore clear that detailed crack initiation and crack propagation mechanisms can be deduced from careful analyses of the fractography of bones via SEM.

4. Nanostructural analysis of bone using transmission electron microscopy

4.1. TEM analyses of fatigue-damage in bone

Bone is one of the few tissues with density high enough to be imaged with transmission electron microscopy (TEM) without staining. TEM is useful in examining the morphological and crystalline arrangement of mineral apatites and crystal–collagen interactions.

TEM analyses of collagen fibrils and apatite crystals in fatigue-damaged bone are limited. Recently, collagen fibrils and apatite crystals in fatigued and non-fatigued murine femora were examined for the ultrastructural damage using high-resolution transmission electron microscopy (HRTEM) (Hong et al., in review; Hong and Kohn, in review). The longitudinally sectioned non-fatigued femora (Fig. 7(a)) displayed well-aligned and uniformly distributed collagen fibrils mostly parallel to the bone axis (indicated by the arrow). In the fatigue-damaged femora (Fig. 7(b)), the aligned arrangement of collagen fibrils appeared to be

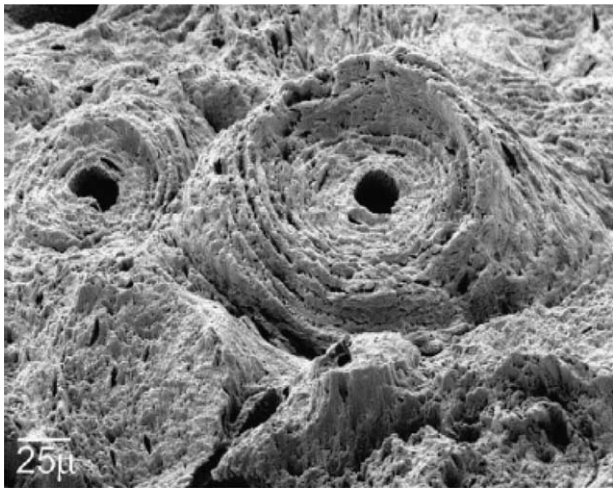

Fig. 6. Scanning electron micrograph of an osteon on the transverse fracture surface of a cyclically loaded dorsal specimen. Disruption of interlamellar and cement line interfaces reveals concentric lamellae and the outer osteon boundary of 'pulled out' osteons. Reprinted from Hiller et al., 2003, with permission from the authors and Elsevier Ltd.

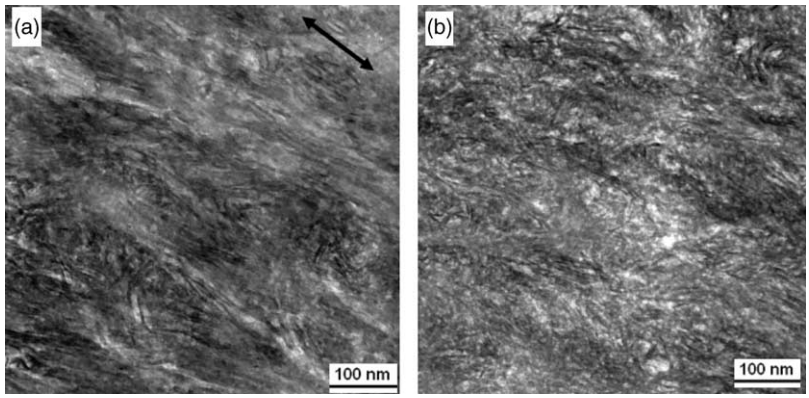

Fig. 7. Ultrastructure of murine lamellar bone before (a) and after (b) fatigue. The non-fatigued femora displayed well-aligned and uniformly distributed collagen fibrils mostly parallel to the bone axis (indicated by the arrow). In the fatigue-damaged femora, the aligned arrangement of collagen fibrils appeared to be impaired and loosened.

impaired and loosened. The damage is manifested by non-uniformly distributed and shorter collagen fibrils, which may have resulted from rearrangement and fragmentation of collagen fibrils in reaction to the applied load. At a higher magnification, HRTEM images of the non-fatigued femora displayed tablet-like crystals with lattice fringes (Hong and Kohn, in review). In the fatigue-damaged femora, crystalline lattice fringes were much less frequently observed and small pieces of particles adjacent to each other were observed (Fig. 8, indicated by arrows). Hong and Kohn (in review) suggested, based on HRTEM images and the presence of diffuse halos in the diffraction patterns that some apatite crystals were broken into small pieces and a fraction of crystalline mineral apatites became amorphous during fatigue. The observation of amorphization represents morphological validation of Raman spectroscopic findings, in which altered Raman signatures at the tips of microcracks were interpreted as evidence of fatigue-induced amorphization (Timlin et al., 2000)

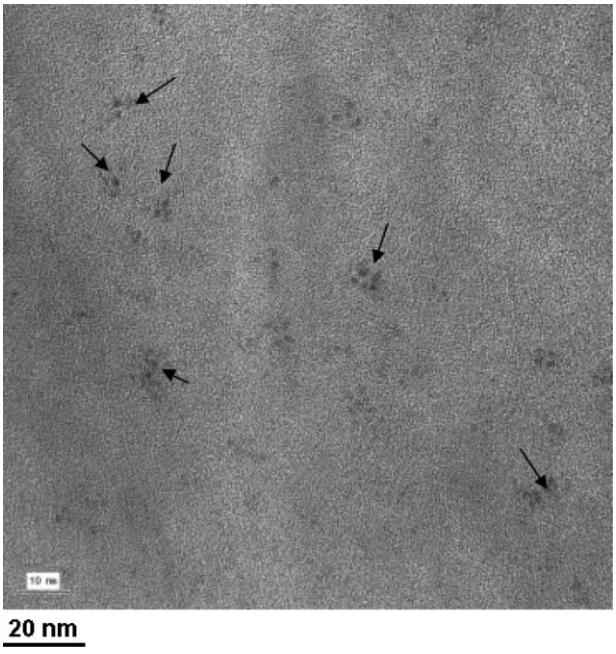

Fig. 8. High-resolution transmission electron microscopic (HRTEM) images of fatigued murine lamellar bone at a high magnification. Small pieces of particles adjacent to each other and some featureless amorphous regions were observed.

The load-carrying capacity of mineral apatites deteriorates following amorphization, and fragmentation, which are likely to trigger the overall fatigue-induced microdamage and microcracks of bones. More detailed analyses using TEM are needed to understand nanostructural damage accumulation mechanisms and their effect on macroscopic failure and bone remodeling.

4.2. TEM analyses of osteoporotic bone

Differences between normal and osteoporotic trabecular bone include lower bone mineral density and trabecular volume, and thinner trabecular struts in osteoporotic bone (Rubin et al., 2003). Relatively few studies, however, have analyzed ultrastructural differences between normal and osteoporotic bone, and the ultrastructural changes in collagen in osteoporotic bone are still under debate. For example, an irregular and random arrangement of collagen fibrils has been noted in osteoporotic bone, compared to the parallel and well-aligned array of fibrils in normal bone (Kafantari et al., 2000). The diameter of collagen fibrils decreases in both trabecular and cortical bone of ovariectomized rats, a finding attributed to defective cross-linking (Kafantari et al., 2000). The reduced diameter and irregular fibril array, along with altered cross-linking may deteriorate the strength of osteoporotic bone. In other studies, however, no appreciable difference in the size, shape and distribution of collagen fibrils between normal and osteoporotic trabecular bone was noted in either rats (Rohanizadeh et al., 2000) or humans (Rubin et al., 2003). The differences in collagen morphology found in different investigations may be due to changes in collagen that occur upon demineralization and whether fibrils were being

analyzed as an isolated matrix phase or as part of a collagen/mineral aggregate.

Regarding the mineral phase of bone, even though many investigators have examined mineral apatites using TEM, there is no consensus about crystallite size in bone. Moreover, there is also a lack of knowledge about the structure of diseased bone, such as osteoporotic bone. For example, three distinct views on the size of osteoporotic bone crystals have been presented: the osteoporotic crystals are either smaller (Grynpas and Holmyard, 1988), of the same size (Rohanizadeh et al., 2000; Rubin et al., 2003; Simmons et al., 1991) or, larger than those in normal bone (Boskey, 1990; Chatterji et al., 1981).

TEM micrographs of the cross-section of mineral/collagen fibril conglomerates demonstrated no appreciable difference in the size, shape and distribution of apatite between normal and osteoporotic trabecular bone in humans (Rubin et al., 2003) or rats (Rohanizadeh et al., 2000). (e.g. Fig. 9). Plate-like and tablet-like crystals with their long axes aligned with the long-axis (*c*-axis) of fibrils were observed in both normal and osteoporotic trabecular bone (Rubin et al., 2003). The length and width of apatite crystals in human osteoporotic trabecular bone in longitudinal section fibrils were 49.8 ± 10.4 and 7.1 ± 1.7 nm, respectively, compared with 50.7 ± 9.1 and 7 ± 1.5 nm in normal bone, supporting no significant difference in length and morphology of apatite crystals between normal and osteoporotic bones. Rubin et al. (2003) therefore suggested that the chief mechanism underlying the lower bone mineral density in osteoporotic bone is a reduction in trabecular volume, rather than a deterioration of the bone crystals at the nanoscale.

It requires caution, however, to interpret data on the size of apatite crystals in osteoporotic bone, because it is difficult to separate effects of age from effects of the disease itself. In addition, a more important feature than the size of apatite crystals in osteoporotic bone may be the local volume density of apatite crystals, which has not been given much attention. Further work directed at analysis of the local volume density of apatite crystals and the relationship between alterations in collagen fibrils and apatite crystals using TEM is needed for a better understanding of osteoporosis and other bone diseases.

5. Spectroscopic imaging of bone

5.1. Compositional parameters affecting bone quality

In engineering composite materials, it is well known that composition has a significant influence on mechanical properties as well as on the spatial and temporal progression of damage accumulation (Matthews and Rawlings, 1994). By analogy, bone may be viewed as a composite (at multiple levels of hierarchy), and its composition as well as architecture (e.g. mineral crystallite size, shape, orientation and specific mineral to mineral and mineral to matrix ratios; collagen fiber organization and orientation; bonding between the mineral and collagen phases, among other parameters) also dictate mechanical performance (Carter and Hayes, 1977a,b; Grynpas and Holmyard, 1988; Currey et al., 1996; Martin et al., 1998; Rho et al., 1998). The compositional and ultrastructural parameters of bone modulate whole bone properties and also play an important role in determining mechanisms of fatigue-induced microdamage (Carter and Hayes, 1977a,b; Grynpas and Holmyard, 1988; Currey et al., 1996; Martin et al., 1998; Rho et al., 1998). These parameters also change with age and are therefore likely contributors to age-related skeletal fragility, which may be reflected first in an increase in local damage and, upon continued growth, a decrease in global mechanical properties (Ruff and Hayes, 1984; Boyde et al., 1993). For example, mineral crystallinity, orientation, and impurity substitution increase with age (Camacho et al.,

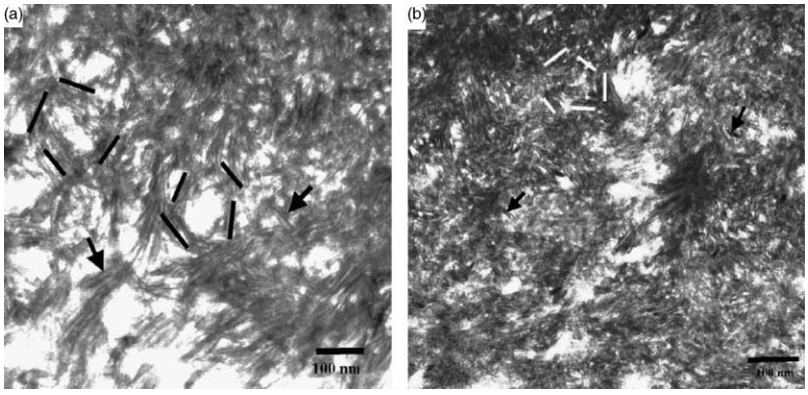

Fig. 9. TEM micrographs of the cross-section of mineral/collagen fibril aggregates in normal (a) and osteoporotic (b) human trabecular bone. Distinct individual hydroxyapatite crystals are seen within the mineral/collagen aggregates as tablet-like (plates on edge) shapes (arrows). Crystal organization in fibrils displayed more of a random undulated arrangement, with localized areas demonstrating circular oriented patterns of only tablet-like crystals patterns (bars indicate orientation of the crystal at that particular location). The orientation of the tablet-like crystals distinctively changes within a 100-200-nm-diameter area. Reprinted from Rubin et al., 2003, with permission from the authors and Elsevier Ltd.

1999). These age-related changes in mineral are also accompanied by an increase in organic phase (i.e. collagen) compaction (Grynpas, 1993). Less rigorously defined, however, are specific associations between local microdamage and local composition of the surrounding tissue matrix. Toward this end, investigators have started to use spectroscopic techniques, primarily Fourier transform infrared spectroscopy (FTIR) and Raman spectroscopy, to relate mechanical history, spatial state of damage and local bone chemistry.

5.2. Vibrational spectroscopy and imaging

Bone mineral spectra observed as Raman-shifted scatter from near-infrared excitation will be found around 850–860 nm, while the infrared absorption spectra will be found around 10–11 μm. Since lateral resolution in optical microscopic imaging is limited by diffraction to about half the observation wavelength, spatial resolution for mineral content is at least 10× better with Raman spectroscopy than with IR spectroscopy, because of the much shorter wavelengths involved in Raman spectroscopy. Spatial resolution is especially important in the imaging of any boundary—such as around an osteon, a cement line or the edge of a crack or fracture, where poor resolution from IR imaging can blur important detail. High resolution (<1 μm) Raman imaging is possible, even with a dry microscope objective.

In bone mineral, there are several slightly different phosphate moieties, depending on the substitution of the matrix near the phosphate. Each different moiety gives rise to a slightly different frequency for the same phosphate vibration. This is why each phosphate band can usually be resolved into two or more components by multivariate analysis techniques. The situation is similar for the matrix bands.

5.3. Spectroscopy of bone

There is a reasonably large literature on vibrational spectroscopy of bone (Carden and Morris, 2000; Penel et al., 1998). The major Raman band assignments for bone (Table 1) include vibrational modes for phosphate, carbonate and mono-hydrogen phosphate. The important matrix bands are mostly markers for the collagen backbone (amide I, 1660 cm^{-1}; methylene (CH_2) wag, 1450 cm^{-1}; amide III, 1260 cm^{-1}). A point Raman spectrum of bone (Fig. 10) also shows the phosphate (PO_4^{-3}) symmetric stretch (ν_1, ca. 960 cm^{-1}), B-type carbonate (CO_3^{-2}) symmetric stretch (ca. 1070 cm^{-1}) and amide I envelope (ca. 1660–1670 cm^{-1}).

Table 1
Raman band assignments and positions

Band assignment	Position, (cm^{-1})
P–O ν_2	422–454
P–O ν_4	578–617
P–O ν_1	957–962
Mono-hydrogen phosphate ν_1	1010
Carbonate ν_1	1065–1071
Amide III	1243–1269
CH_2 wag	1447–1452
Amide I	1660–1671

The positions, intensities and widths of PO_4^{-3} and CO_3^{-2} bands change in response to local perturbations to the crystal structure caused by the local ion composition; therefore, vibrational spectroscopy is a sensitive probe of the changes in the environment of the molecule. The band positions, intensities and shapes report on the state of maturation as well as on abnormal composition resulting from genetic defects or disease. Vibrational spectroscopy therefore allows convenient measurement of mineral/matrix ratios, as well as alterations in mineral content associated with aging and/or mechanical deformation.

5.4. Chemical changes associated with damage and deformation in bone

A Raman image of a small region of bovine femoral cortical bone that had been loaded in fatigue, stained en-bloc with basic fuchsin and histologically analyzed for microdamage shows spectra despite the presence of basic fuchsin, a stain that has appreciable fluorescence in the visible wavelengths (Fig. 11(b)). An unusually high frequency component to the phosphate ν_1 band (963 cm^{-1}), corresponding to uncarbonated apatite, appears in the region of microcracks (Timlin et al., 2000). The high-frequency component was not seen in undamaged areas (Fig. 11(a)). This data did not determine whether the altered phosphate chemistry was a cause or result of the microdamage, but did provide evidence that compositional changes are associated with regions of damage.

Following the observation of an association between local chemical changes and local microfractures, the hypothesis that mechanical loading leads to these chemical changes was addressed by performing experiments in which bones were loaded and spectra were collected in near real-time (Morris et al., 2001; de Carmejane et al., 2005). Under compressive loading that ranged up to 1% strain, a change in the PO_4^{3-} peak center of gravity was observed (Morris et al., 2001). A smaller and more transient change was observed in the carbonate bands. A considerable shift in the amide I band was observed (Morris et al., 2001), confirming that the matrix is also influenced by mechanical load. The fact that these changes in mineral and matrix were observed as functions of increasing stress and strain indicates that loading drives the chemical shifts, not that local deformation preferentially occurs at sites of altered chemistry.

Recent indentation experiments also provide convincing evidence that stress causes mineral phase changes (Carden et al., 2003). Cylindrical indents of 100–400 μm depth and 500 μm diameter were made in bovine cortical tissue using

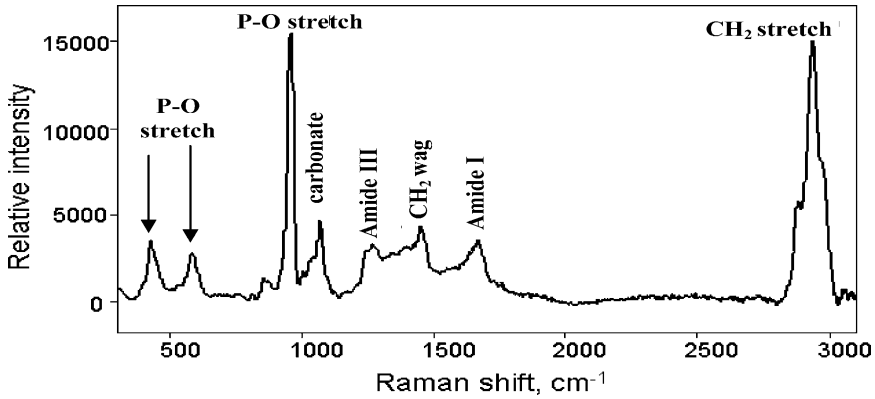

Fig. 10. Raman spectrum of bovine cortical bone taken on a near-IR optimized system, identifying mineral matrix bands of importance, Courtesy Kaiser Optical Systems, Inc., Ann Arbor, Michigan, USA.

pressures of 0.4–1.4 GPa for 10 s. New mineral factors were observed within the indents, up to the walls. Within 20 μm of the walls, but not in the center of the indents, we observed rupture of collagen cross-links as high frequency shoulders on the collagen amide I envelope. Collectively, this data supports stress-induced crystal structure changes in bone mineral as a mechanism of ultrastructural response to loading.

Similar phenomena were observed in 4-month-old mouse femora subjected to bending (Morris et al., 2002). Factor analysis of 4-month-old specimens revealed only one type of mineral present, a carbonated hydroxyapatite-like mineral. However, when the same specimens were loaded and re-imaged, they showed two distinct mineral species: a carbonated HAP-like mineral and an uncarbonated mineral with a high-frequency phosphate component. This two-component composition was observed in all 4 month fractured specimens near the site of fracture, while the control specimens showed only one mineral component. These results are consistent with the hypothesis that the stress leading to fracture caused a phase transformation within the bone mineral lattice which was easily found using Raman imaging. Interestingly and importantly, this effect was not observed in older (18 month) tissue. Factor analysis of images of control and fractured femora in this age group showed only one mineral component occurring in both fractured and unfractured bone. It is therefore possible that there are age-related differences in the mineral's response to stress. Older mineral tends to have more uniform crystallite sizes (Rey et al., 1991; Paschalis et al., 1997); this may affect its reaction to applied load.

6. Summary

Gaining insight into the mechanisms of fracture and how these mechanisms are modulated by intrinsic (e.g. aging and disease) and extrinsic (e.g. mechanical loading) factors may improve the ability to define fracture risk and develop and assess preventative therapies for skeletal fractures. Insight into failure mechanisms of bone, particularly at the ultrastructural-level, is facilitated by the development of improved means of defining and measuring tissue quality. In particular, high resolution microscopy, including scanning and transmission electron microscopies, and spectroscopic imaging techniques (FTIR and Raman) allow for a direct observation of crack initiation and growth, and are valuable for deciphering incipient mechanisms of failure. Collectively, the information gained from these techniques can compliment mechanical and histological assays leading to a more complete understanding of fragility.

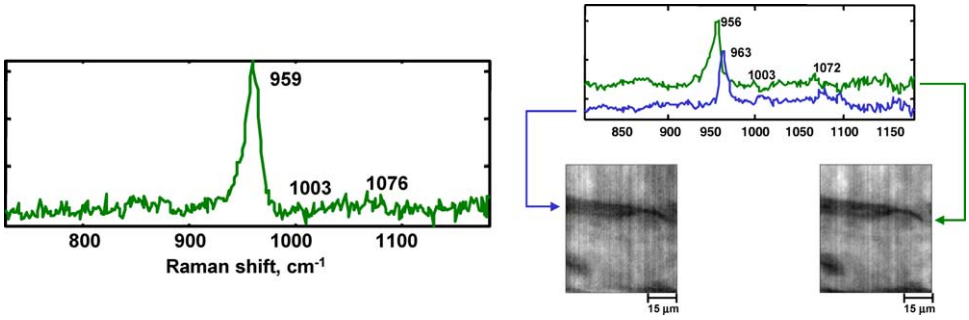

Fig. 11. Raman Spectra for undamaged ((a), left) and damaged (microcracked) regions ((b), right) of bovine cortical bone. Factor analysis revealed an additional high frequency phosphate species in cracked regions. Score images reveal the spatial distribution of these two mineral factors. From Timlin et al., 2000, with permission.

Acknowledgements

We acknowledge support from US Department of Defense/Department of the Army DAMD17-03-1-0556 (DHK). SIH is grateful for the support from Korea Research Foundation (2004-D00318).

References

Akkus, O., Rimnac, C.M., 2001. Cortical bone tissue resists fatigue fracture by deceleration and arrest of microcrack growth. Journal of Biomechanics 34, 757–764.

Beck, T.J., Ruff, C.B., Shaffer, R.A., 2000. Stress fracture in military recruits: Gender differences in muscle and bone susceptibility factors. Bone 27, 437–444.

Bennell, K.L., Malcolm, S.A., Thomas, S.A., 1996. Risk factors for stress fractures in track and field athletes: a twelve month prospective study. American Journal of Sports Medicine 24, 810–818.

Birdwood, G., 1996. Understanding Osteoporosis and its Treatment, A Guide for Physicians and their Patients. Pearl River, New York.

Boskey, A.L., 1990. Bone mineral and matrix: Are they altered in osteoporosis? Orthopaedic Clinics of North America 21, 19–29.

Boyce, T.M., Fyhrie, D.P., Glotkowski, M.C., Radin, E.L., Schaffler, M.B., 1998. Damage type and strain mode associations in human compact bone bending fatigue. Journal of Orthopaedic Research 16, 322–329.

Boyde, A., Elliott, C., Jones, S.J., 1993. Stereology and histogram analysis of backscattered electron images: Age changes in bone. Bone 14, 205–210.

Braidotti, P., Bemporad, E., D'Alessio, T., Sciuto, S.A., Stagni, L., 2000. Tensile experiments and SEM fractography on bovine subchondral bone. Journal of Biomechanics 33, 1153–1157.

Burr, D.B., 1997. Bone, exercise and stress fractures. Exercise Science and Sports Review 25, 171–194.

Burr, D.B., Stafford, T., 1990. Validity of the bulk-staining technique to separate artifactual from in vivo bone microdamage. Clinical Orthopaedics and Related Research 260, 305–308.

Burr, D.B., Milgrom, C. (Eds.), 2001. Musculoskeletal Fatigue and Stress Fractures. CRC Press, Boca Raton, FL.

Burr, D., Forwood, M., Fyhrie, D., Martin, R., Schaffler, M., Turner, C., 1997. Bone microdamage and skeletal fragility in osteoporotic and stress fractures. Journal of Bone and Mineral Research 12, 6–15.

Burr, D.B., Turner, C.H., Naick, P., Forwood, M.R., Ambrosius, W., Hasan, M.S., Pidaparti, R., 1998. Does microdamage accumulation affect the mechanical properties of bone? Journal of Biomechanics 31, 337–345.

Burr, D.B., Turner, C., Forwood, M.R., Pidaparti, R., 1999. Quantification of bone damage and crack morphology and its effect on skeletal fragility: Response to Zioupos. Journal of Biomechanics 32, 213–215.

Camacho, N.J., Rinnerthaler, S., Paschalis, E.P., Mendelsohn, R., Boskey, A.L., Fratzl, P., 1999. Complementary information on bone ultrastructure from scanning small angle X-ray and Fourier transform infrared microspectroscopy. Bone 25, 287–293.

Carden, A., Morris, M.D., 2000. Application of vibrational spectroscopy to the study of mineralized tissues. Journal of Biomedical Optics 5, 259–268.

Carden, A., Morris, M.D., Rajachar, R.M., Kohn, D.H., 2003. Ultrastructural changes in the mechanical deformation of bone tissue: A raman imaging study. Calcified Tissue International 72, 166–175.

Carter, D.R., Hayes, W.C., 1977a. Compact bone fatigue damage: A microscopic examination. Clinical Orthopaedics and.Related Research 127, 265–274.

Carter, D.R., Hayes, W.C., 1977b. Compact bone fatigue damage—I. Residual strength and stiffness. Journal of Biomechanics 10, 325–337.

Chatterji, S., Wall, J.C., Jefferey, J.W., 1981. Age related changes in the orientation and particle size of the mineral phase in human cortical bone. Calcified Tissue International 33, 567–574.

Colopy, S.A., Benz-Dean, J., Barrett, J.G., Sample, S.J., Lu, Y., Danova, N.A., Kalscheur, V.L., Vanderby Jr., R., Markel, M.D., Muir, P., 2004. Response of the osteocyte syncytium adjacent to and distant from linear microcracks during adaptation to cyclic fatigue loading. Bone 35, 881–891.

Courtney, A.C., Hayes, W.C., Gibson, L.J., 1996. Age-related differences in post-yield damage in human cortical bone. experiment and model. Journal of Biomechanics 29, 257–260.

Currey, J.D., 2003. The many adaptations of bone. Journal of Biomechanics 36, 1487–1495.

Currey, J.D., Brear, K., Zioupos, P., 1996. The effects of ageing and changes in mineral content in degrading the toughness of human femora. Journal of Biomechanics 29, 257–260.

Danova, N.A., Colopy, S.A., Radtke, C.L., Kalscheur, V.L., Markel, M.D., Vanderby, R., McCabe, R.P., Escarcega, A.J., Muir, P., 2003. Degradation of bone structural properties by accumulation and coalescence of microcracks. Bone 33, 197–205.

de Carmejane, O., Morris, M.D., Davis, M.K., Stixrude, L., Tecklenburg, M., Rajachar, R.M., Kohn, D.H., 2005. Bone chemical structure response to mechanical stress studied by high pressure raman spectroscopy. Calcified Tissue International 76, 207–213.

Fazzalari, N.L., Forwood, M.R., Manthey, B.A., Smith, K., Kolesik, P., 1998. Three-dimensional confocal images of microdamage in cancellous bone. Bone 23, 373–378.

Frost, H.M., 1960. Presence of microscopic cracks in vivo in bone. Bulletin of the Henry Ford Hospital 8, 25–35.

Goldstein, J.I., Newbury, D.E., Echlin, P., Joy, D.C., Fiori, C., Lifshin, E., 1981. Scanning Electron Microscopy and X-ray Microanalysis. Plenum Press, New York.

Griffin, L.V., Gibeling, J.C., Martin, R.B., Gibson, V.A., Stover, S.M., 1997. Model of flexural fatigue damage accumulation for cortical bone. Journal of Orthopaedic Research 15, 607–614.

Grynpas, M.D., Holmyard, D., 1988. Changes in quality of bone mineral on aging and in disease. Scanning Microscopy 2, 1045–1054.

Grynpas, M., 1993. Age and disease-related changes in post-yield damage in human cortical bone. Calcified Tissue International 53, S57–S64.

Hiller, L.P., Stover, S.M., Gibson, V.A., Gibeling, J.C., Prater, C.S., Hazelwood, S.J., Yeh, O.C., Martin, R.B., 2003. Osteon pullout in the equine third metacarpal bone: Effects of ex-vivo fatigue. Journal of Orthopaedic Research 21, 481–488.

Hong, S.I., Suryanarayana, C., 2001. Is ductilization of intermetallic compounds by nanostructure processing a possibility? Materials Transactions 42, 502–508.

Hong, S. I., Kohn, D. H., 2005. Nanostructural analysis of murine femoral trabecular bone, in review.

Hong, S.I., Gray, G.T., Wang, Z., 1996. Microstructure and stress-strain response of Al-Mg-Si alloy composites reinforced with 15% Al2O3. Materials Science and Engineering 221, 38–47.

Hong, S. I., Hong, S. K., Kohn, D. H., 2005. Fatigue induced damage of mineral apatites in murine femoral bone, in review.

Hui, S., Slemenda, C., Johnston, C., 1988. Age and bone mass as predictors of fracture in a prospective study. Journal of Clinical Investigation 81, 1804–1809.

Jones, B.H., Harris, J.M., Vinh, T.N., Rubin, C., 1989. Exercise-induced stress fractures and stress reactions of bone: Epidemiology, etiology and classification. Exercise Sport Science Reviews 17, 379–422.

Jordaan, G., Schwellnus, M.P., 1994. The incidence of overuse injuries in military recruits during basic military training. Military Medicine 159, 421–426.

Kafantari, H., Kounadi, E., Fatouros, M., Milonakis, M., Tzaphlidou, M., 2000. Structural alterations in rat skin and bone collagen fibrils induced by ovariectomy. Bone 26, 349–353.

Lee, K.H., Hong, S.I., 2003. Interfacial and twin boundary structures of nanostructured filamentary composites. Journal of Materials Research 18, 2194–2202.

Martin, R.B., Burr, D.B., Sharkey, N.A., 1998. Skeletal Tissue Mechanics. Springer Verlag, New York.

Matthews, F., Rawlings, R., 1994. Composite Materials: Engineering and Science. Chapman and Hall, New York.

Morris, M.D., Carden, A., Rajachar, R.M., Kohn, D.H., 2001. Bone microstructure deformation observed by raman microscopy. In: Vo-Dinh, T. et al. (Ed.), Biomedical Diagnostic, Guidance, and Surgical-Assist Systems III, 4254. Society for Optical Instrumentation and Engineering (SPIE) Press, Bellingham, WA, pp. 81–89.

Morris, M.D., Carden, A., Rajachar, R.M., Kohn, D.H., 2002. Effects of applied load on bone tissue as observed by raman spectroscopy. In: Mahadevan-Jansen, A. (Ed.), Biomedical Vibrational Spectroscopy II, vol. 4614. Society for Optical Instrumentauion and Engineering (SPIE) Press, Bellingham, WA, pp. 47–54.

Nalla, R.K., Kinney, J.H., Ritchie, R.O., 2003. Mechanistic fracture criteria for the failure of human cortical bone. Nature Materials 2, 164–168.

Nalla, R.K., Kruzic, J.J., Ritchie, R.O., 2004. On the origin of the toughness of mineralized tissue: Microcracking or crack bridging? Bone 34, 790–798.

National Osteoporosis Foundation, Annual Report, 2001 (http://www.nof.org).

Norman, T.L., Wang, Z., 1997. Microdamage of human cortical bone: incidence and morphology in long bones. Bone 20, 375–379.

Norman, T.L., Yeni, Y.N., Brown, C.U., Wang, Z., 1998. Influence of microdamage on fracture toughness of the human femur and tibia. Bone 23, 303–306.

O'Brien, F.J., Taylor, D., Lee, T.C., 2003. Microcrack accumulation at different intervals during fatigue testing of compact bone. Journal of Biomechanics 36, 973–980.

Paschalis, E.P., Betts, F., DiCarlo, E., Mendelsohn, R., Boskey, A.L., 1997. FTIR microspectroscopic analysis of normal human cortical and trabecular bone. Calcified Tissue International 61, 480–486.

Penel, G., Leroy, G., Rey, C., Bres, E., 1998. MicroRaman spectral study of the PO4 and CO3 vibrational modes in synthetic and biological apatites. Calcified Tissue International 63, 475–481.

Praemer, A., Furner, S., Rice, D.P., 1999. Musculoskeletal Conditions in the United States. American Academy of Orthopaedic Surgeons, Rosemont, IL.

Rajachar, R.M., 2003. Effects of age-related ultrastructural level changes in bone on microdamage mechanism, Ph.D. Thesis, University of Michigan.

Reilly, G.C., 2000. Observations of microdamage around osteocyte lacunae in bone. Journal of Biomechanics 33, 1131–1134.

Reilly, G.C., Currey, J.D., 2000. The effects of damage and microcracking on the impact strength of bone. Journal of Biomechanics 33, 337–343.

Rey, C., Renugopalakrishnan, Collins, B., Glimcher, M.J., 1991. Fourier transform infrared spectroscopic study of the carbonate ions in bone mineral during aging. Calcified Tissue International, 251–258.

Rho, J.-Y., Kuhn-Spearing, L., Zioupos, P., 1998. Mechanical properties and the hierarchial structure of bone. Medical Engineering and Physics 20, 92–102.

Rohanizadeh, R., LeGeros, R.Z., Bohie, S., Pilet, P., Barbier, A., Daculsi, G., 2000. Ultrastructural properties of bone mineral of control and tiludronate-treated osteoporotic rat. Calcified Tissue International 67, 330–336.

Rubin, M.A., Jasiuk, I., Taylor, J., Rubin, J., Ganey, T., Apkarian, R.P., 2003. TEM analysis of the nanostructure of normal and osteoporotic human trabecular bone. Bone 33, 270–282.

Ruff, C.B., Hayes, W.C., 1984. Age changes in geometry and mineral content of the lower limb bones. Annals of Biomedical Engineering 12, 573–584.

Schaffler, M.B., Radin, E.L., Burr, D.B., 1989. Mechanical and morphological effects of strain rate on fatigue of compact bone. Bone 10, 207–214.

Schaffler, M.B., Pitchford, W.C., Choi, K., Riddle, J.M., 1994. Examination of compact bone microdamage using back-scattered electron microscopy. Bone 15, 483–488.

Schaffler, M.B., Choi, K., Milgrom, C., 1995. Aging and matrix microdamage accumulation in human compact bone. Bone 17, 521–525.

Simmons Jr.., E.D., Pritzker, K.P.H., Grynpas, M.D., 1991. Age-related changes in human femoral cortex. Journal of Orthopaedic Research 9, 155–167.

Sobelman, O.S., Gibeling, J.C., Stover, S.M., Hazelwood, S.J., Yeh, O.C., Shelton, D.R., Martin, R.B., 2004. Do microcracks decrease or increase fatigue resistance in cortical bone? Journal of Biomechanics 37, 1295–1303.

Timlin, J.A., Carden, A., Morris, M.D., Rajachar, R.M., Kohn, D.H., 2000. Raman spectroscopic markers for fatigue-related bovine bone microdamage. Analytical Chemistry 72, 2229–2236.

Vashishth, D., Behiri, J.C., Bonfield, W., 1997. Crack growth resistance in cortical bone: Concept of microcrack toughening. Journal of Biomechanics 30, 763–769.

Vashishth, D., Koontz, J., Qiu, S.J., Lundin-Cannon, D., Yeni, Y.N., Schaffler, M.B., Fyhrie, D.P., 2000a. In vivo diffuse damage in human vertebral trabecular bone. Bone 26, 147–152.

Vashishth, D., Tanner, K.E., Bonfield, W., 2000b. Contribution, development and morphology of microcracking in cortical bone during crack propagation. Journal of Biomechanics 33, 1169–1174.

Vashishth, D., Tanner, K.E., Bonfield, W., 2003. Experimental validation of a microcracking-based toughening mechanism for cortical bone. Journal of Biomechanics 36, 121–124.

Weiner, S., Traub, W., Wagner, H.D., 1999. Lamellar bone: Structure-function relations. Journal of Structural Biology 126, 241–255.

Zioupos, P., 1999. On microcracks, microcracking, in-vivo, in vitro, in-situ and other issues. Journal of Biomechanics 32, 209–211. 213–59.

Zioupos, P., Currey, J.D., 1998. Changes in the stiffness, strength and toughness of human cortical bone with age. Bone 22, 57–66.